Malaysian Journal of Catalysis
http://mjcat.utm.my/
MJCat Research Article

Effect of Ni/Al-MCM-41 Impregnation Method on Catalytic Deoxygenation of Reutealis Trisperma Oil

Reva Edra Nugraha[1]*, Rida Kharismawati[2], Suprapto Suprapto[2], Abdul Aziz[3], Holilah Holilah[4,5], Hartati Hartati[6], Didik Prasetyoko[2*]

[1]*Department of Chemical Engineering, Faculty of Engineering, Universitas Pembangunan Nasional "Veteran" Jawa Timur, Surabaya, East Java, 60294, Indonesia*
[2]*Department of Chemistry, Faculty of Science and Data Analytics, Institut Teknologi Sepuluh Nopember, Keputih, Sukolilo, Surabaya, 60111, Indonesia*
[3]*Department of Pharmacy, Kader Bangsa University, Palembang, South Sumatera, 30253, Indonesia*
[4]*Research Center for Biomass and Bioproducts, National Research and Innovation Agency of Indonesia (BRIN), Cibinong, 16911, Indonesia*
[5]*Department of Food Science and Technology, Faculty of Agriculture, Halu Oleo University, Indonesia*
[6]*Department of Chemistry, Faculty of Science and Technology, Universitas Airlangga, Surabaya, 60115, Indonesia*

**Corresponding Author: reva.edra.tk@upnjatim.ac.id; didikp@chem.its.ac.id*

Article history:
Received 11 June 2023
Accepted 01 August 2023

ABSTRACT

Deoxygenation of Reutealis trisperma oil into green diesel has been carried out using Ni/Al-MCM-41 catalyst. The Ni/Al-MCM-41 catalyst was prepared using the wetness impregnation and incipient wetness impregnation methods, hereinafter referred to as Ni/Al-MCM-41 (WI) and Ni/Al-MCM-41 (IWI). XRD and FTIR analysis shows a characteristic of the amorphous phase for solid Al-MCM-41 catalyst. FTIR pyridine was used to assess the impact of the NiO impregnation technique on Lewis acid and Brønsted acidity. The acidity test showed that the Ni/Al-MCM-41 (WI) catalyst had the highest total acidity 0.227 mmol/g. The catalytic activity of Ni/Al-MCM-41 catalyst was examined in the deoxygenation reaction of Reutealis trisperma oil under inert conditions for 4 hours. In comparison to Ni/Al-MCM-41(IWI) and Al-MCM-41 catalysts, the Ni/Al-MCM-41(WI) catalyst produced better results in the deoxygenation reaction of Reutealis trisperma oil. Impregnation with WI method gives higher Lewis acidity which results in increasing RTO conversion via the deoxygenation reaction pathway and suppresses the cracking reaction. Consequently, intensify the green diesel (C11-18) hydrocarbon products with selectivity of 100% and a degree of deoxygenation of 92.77%.

Keywords: *Deoxygenation, Al-MCM-41, Impregnation, Hydrocarbon*

| eISSN 0128-2581 |

1. INTRODUCTION

The development of renewable alternative energy was getting immersive attentions due to the depletion of fossil fuels [1]. An alternative fuel called biodiesel is typically produced by transesterification and esterification processes between oil and alcohol in the presence of catalyst. A number of biodiesel's downsides include poor storage stability, less steady flow properties in cold conditions, limited oxidation stability, and a low cetane value [2]. Fatty acids can be transformed into more stable straight-chain alkanes, such as green diesel, to overcome the biodiesel weakness. The advantages green diesel includes the production of oxygen-free hydrocarbons (high oxidation stability), complete combustion, high energy density, low by-product production and improved performance in cold temperatures [3].

The raw material often used in the production of green diesel is vegetable oil i.e., jatropha oil [4], waste cooking oil [5], ceiba oil, sterculia oil [6], microalgae [7], fallopian japonica oil [8] etc. Sources of non-food vegetable oils (non-edible oil) such as Reutealis trisperma oil are found in many regions of Indonesia. Reutealis trisperma oil is regarded as a viable raw material because of its high oil content (38–40%) and excellent productivity (3.8–7.7 tons/ha/year) [9]. Vegetable oil can be converted into green diesel fuel via catalytic cracking, hydrotreating, and deoxygenation [10,11]. Deoxygenation reactions provide several advantages over hydroprocessing processes for the vegetable oils conversion including high yield production, faster reactions and majority fraction produced is a hydrocarbon group [4].

Zeolites like H-ZSM-5 [12], Y-zeolite [13] and H-β [14] as well as mesoporous materials like MCM-41 [15]and

SBA-15 [16] are a few types of catalysts that can be used in deoxygenation reactions. Mesoporous Al-MCM-41 increased the conversion of Jatropha curcas oil to long-chain (C_{11}-C_{18}) green diesel hydrocarbons, as we have previously reported [17,18]. The strong acidity has an advantage because it speeds up the isomerization reaction and improves the fuel's quality.

In many different catalytic reactions, impregnation of transition metal has been extensively used. Metal oxides can have an impact on the catalytic efficacy and stability of the catalyst, resulting in enhanced conversion, selectivity, and reaction yield [19]. Ni metal oxide is widely used in catalysts due to its less expensive and more plentiful than precious metals [16]. The synthesis of Al-MCM-41 material impregnated in two distinct ways was performed in this study to test its effect on the deoxygenation reaction of Reutealis trisperma oil.

2. EXPERIMENTS

2.1 Synthesis of Al-MCM-41

The hydrothermal approach was utilized to synthesis Al-MCM-41 with the mole ratio of $10Na_2O$: $100SiO_2$: $2Al_2O_3$: $1800H_2O$. The synthesis of Al-MCM-41 in this study utilized kaolin as a source of silicate (SiO_2) and aluminate (Al_2O_3). NaOH was dissolved with distilled water and stirred for 30 minutes. Kaolin is added to the NaOH solution with faster stirring. Add LUDOX and distilled water gently while swirling vigorously after creating the sol. At room temperature for eight hours, the sol mixture was agitated to homogeneity. The product was subsequently put through a six-hour at 70 °C for aging process. The first hydrothermal process was then carried out at 80 °C for 12 hours, and the crystallization process was then stopped by cooling the mixture with running water. The CTAB was added gradually with continuously stirring. At 150 °C for 24 hours, the second hydrothermal procedure was conducted. The hydrothermal gel that resulted was neutralized with distilled water to a pH of 7, then dried for 24 hours at 60 °C in the oven. The dry solid is then calcined at 550 °C (2 °C/min) for 1 hour with N_2 gas flow and followed by 6 hours with air flow.

2.2 Synthesis of Ni/Al-MCM-41

Catalyst Al-MCM-41 was used as support and nickel as impregnated metal with the content of 10%. In this study, the efficacy of two impregnation methods; wet impregnation and incipient wetness impregnation was evaluated.

The first impregnation method was carried out by the wet impregnation method which adapted from Baharudin et. al., (2019) [16]. Firstly, a 10 mL solution of a 1:1 ethanol-water ratio was used to dissolve 0.49 grams of Ni $(NO_3)_2.6H_2O$. After being thoroughly blended, 0.9 gram of Al-MCM-41 was added and swirled for three hours at room temperature. The solution is then gradually heated to 80 °C with continuously stirring and a pale green suspension remained. After that, it was dried for 24 hours at 80 °C in the oven and calcined at 550 °C (2 °C/min) for 1 hour with N_2 gas followed by air flow for for 6 hours with air flow. The wet-impregnated sample is referred to as Ni/Al-MCM-41 (WI).

The incipient wetness impregnation procedure was carried out by dissolving 0.49 grams of Ni $(NO_3)_2.6H_2O$ in 1 mL of a 1:1 ethanol-water solution until homogenous. The nickel nitrate solution was then added dropwise while stirring into 0.9 grams of Al-MCM-41. The nickel nitrate is applied until the entire supporting surface is soaked. Stirring was done for 2 hours, followed by drying in an oven at 80°C for 24 hours. The dry solid was then calcined at 550°C (2°C/min) under N_2 gas flow for 1 hour, followed by air flow for 6 hours. The wet impregnated sample is referred to as Ni/Al-MCM-41 (IWI).

2.3 Catalyst Characterization

X-ray Diffraction (XRD) characterization utilizing a PHILIPS-binary XPert with MPD diffractometer with Cu K radiation operating at 30 mA and 40 kV was used to examine the phase transformation of kaolin to aluminosilicate structure and Ni deposition on catalyst support. Shimadzu Instrument Spectrum One 8400S's Fourier Transform Infra-Red (FTIR) within range of 400-1400 cm^{-1} measurement was used to examine the functional group of catalyst. FTIR Spectroscopy was also used to determine Brønsted and Lewis acid sites in Ni/Al-MCM-41 and Al-MCM-41.

2.3 Catalytic Activity

A 100 mL-3 neck flask with a simple distillation apparatus and a heating mantle was used for the deoxygenation reaction of Reutealis trisperma oil. Prior to the reaction, 0.3 gram of catalyst was added to 10 grams of Reutealis trisperma oil and flowed with N_2 gas to create an inert atmosphere for the reaction. The mixture was then heated to 350 °C with continuously stirring and N_2 was flowing for 4 hours. The yield and conversion of the reaction can be determined from the reaction's results using Equations (1) and (2).

$$Liquid\ yield\ (\%) = \left(\frac{weight\ of\ liquid\ product}{weight\ of\ reactant}\right) x100\% \quad \text{Eq. 1}$$

$$Conversion\ (\%) = \left(\frac{weight\ of\ initial\ reactant - weight\ of\ final\ reactant}{weight\ of\ initial\ reactant}\right) x100\% \quad \text{Eq. 2}$$

The liquid deoxygenated product was then examined with GC-MS (Gas Chromatography-Mass Spectrometry). Equations (3) and (4) can be used to calculate the degree of deoxygenation and product selectivity.

$$Degree\ of\ deoxygenation = \left[1 - \left(\frac{\%FA\ in\ liquid\ product}{\%FA\ in\ reactant}\right)\right] x100\% \quad \text{Eq. 3}$$

$$Selectivity = \frac{(peak\ area\ of\ desired\ hydrocarbon)}{(peak\ area\ of\ total\ hydrocarbon)}\ x\ 100\% \quad \text{Eq.4}$$

3. RESULTS AND DISCUSSION

3.1 XRD Analysis

In this study, XRD analysis was performed with the range of 2θ=5- 50° for Al-MCM-41 and 2θ=5-80° for Ni/Al-MCM-41. The diffraction pattern of Al-MCM-41 and Ni/Al-MCM-41 were shown in Figure 1 dan Figure 2. The characteristic peak of the Al-MCM-41 material may be seen in the diffractogram of the material at 2θ=15–30°. This peak suggests the presence of an amorphous phase in the Al-MCM-41 material [20,21]. The impregnated Ni on Al-MCM-41 catalyst exhibits additional peaks at 2θ= 37°, 43°, 62°, and 75° which are associated with the diffraction planes (111), (210) (220), and (311) of face-centered cubic NiO [22,23]. The presence of the characteristic NiO peak shows that NiO was impregnated successfully on the surface of Al-MCM-41 [4].

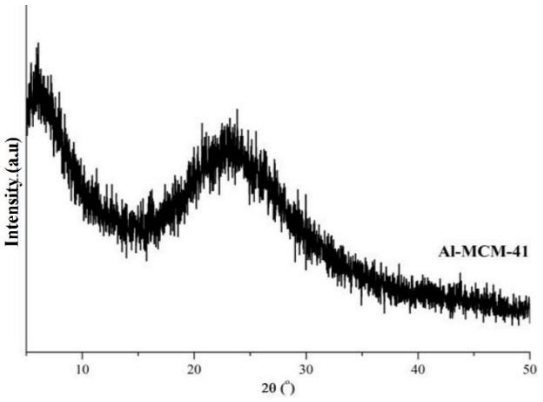

Figure 1. Diffraction pattern of Al-MCM-41

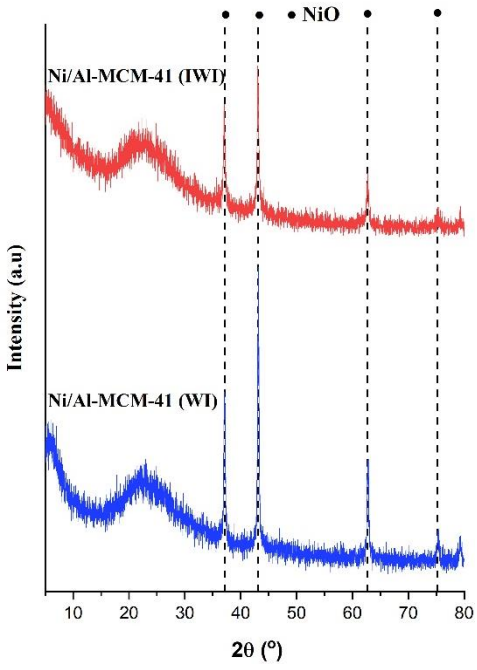

Figure 2. Diffraction pattern of Ni/Al-MCM-41

Table 1 displays the NiO crystallite sizes for both Ni/Al-MCM-41 catalysts which were determined using the Debye Scherrer equation at 2θ=37° (111). In contrast to Ni/Al-MCM-41(IWI), NiO particles are smaller in the Ni/Al-MCM-41(WI) catalyst. The variation in crystal size reveals the impregnation technique affected nickel dispersion in the Al-MCM-41 catalyst.

Table 1. Crystallite size NiO with Debye Scherrer equation

Catalyst	2θ (°)	FWHM (rad)	B (°)	d (nm)
Ni/Al-MCM-41 (IWI)	37.0558	0.1004	0.001752	83.4
Ni/Al-MCM-41 (WI)	37.0661	0.1506	0.002628	55.5

3.2 FTIR Analysis

The FTIR spectra of Al-MCM-41 was shown in Figure 3. Five distinctive absorption peaks were detected from Al-MCM-41 catalyst. The asymmetric stretching of Si–O–Si bands was appeared in absorption band of 1234 cm^{-1} [22,24]. The peak at 470 cm^{-1} is due to the T-O bond's bending vibrations, where T is an atom of Si or Al. Si-O-Si vibration exhibits an internal asymmetric stretching vibration at wave number 1100 cm^{-1}, while Si-O-Al bonds are present at wave number 799 cm^{-1}. A mesoporous structure characteristic is shown by the peak at wave number 968 cm^{-1}, which is caused by the vibration of silanol groups (Si-OH).

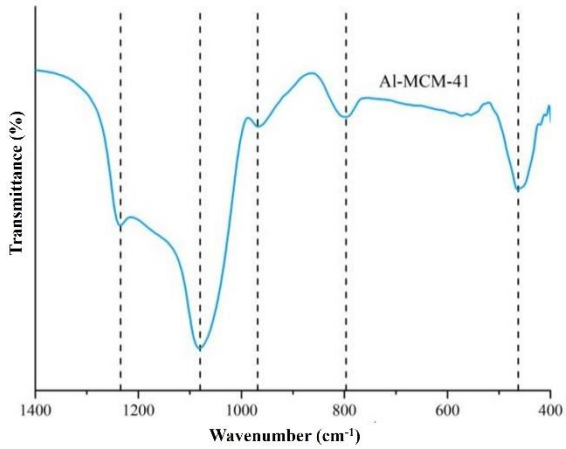

Figure 3. FTIR spectra of Al-MCM-41

3.3 Catalyst Acidity

The pyridine adsorption FTIR was used to determine the number and kind of acid sites on the catalyst. The pyridine-FTIR spectra of all samples show three adsorption peaks at 1446, 1490 and 1546 cm^{-1} which correlated to Lewis and Brønsted acid sites [25,26]. The adsorption peak at 1446 cm^{-1} was generated due to the transferring electron

pairs from the secondary amine group in pyridine to Lewis acid sites in the catalyst. Meanwhile, adsorption at 1546 cm^{-1} correspond to proton transfer from Brønsted acid sites to form a pyridinium ion ($C_5H_5NH^+$) with a pyridine molecule [27]. The adsorption peak at wave number 1490 cm^{-1} associated to the total peak of both Lewis acid and Brønsted acid sites.

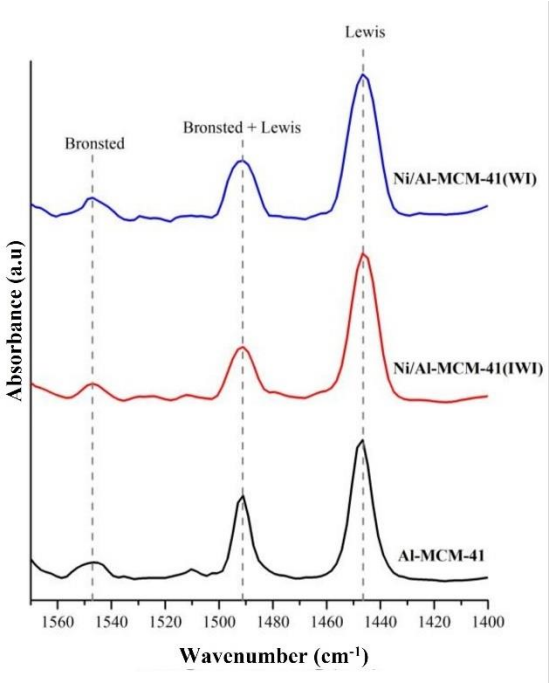

Figure 4. Pyridine-FTIR spectra of Al-MCM-41 and Ni/Al-MCM-41

The number of acid Al-MCM-41 and Ni/Al-MCM-41 catalysts was summarized in Table 2. The acidity of the Lewis acid sites increases with a trend of Ni/Al-MCM-41(WI)>Ni/Al-MCM-41(IWI)>Al-MCM-41. This implies an effect of NiO addition to the quantity of Lewis acid. The inclusion of NiO, on the other hand, reduces the amount of Brønsted acid sites. The decrease in Brønsted acid on the Ni/Al-MCM-41 catalyst was caused by proton exchange of Ni^{2+} ions from NiO from Si-O-Al framework [16].

Table 2. Number of Brønsted and Lewis acid sites of catalysts

Catalysts	Acid Sites (mmol/g)		Lewis+ Brønsted (mmol/g)
	Lewis	Brønsted	
Al-MCM-41	0.154	0.042	0.196
Ni/Al-MCM-41 (IWI)	0.168	0.028	0.197
Ni/Al-MCM-41 (WI)	0.196	0.031	0.227

3.4 Catalytic Activity

The catalytic activity was tested in the deoxygenation reaction of Reutealis trisperma oil. The deoxygenation reaction was carried out for 4 hours at 350 °C with a N_2 gas flow. In this catalytic activity test, the GC-MS instrument was utilized to perform qualitative and quantitative analysis on the deoxygenation process product. The conversion, yield and degree of deoxygenation of liquid product obtained from different catalysts was shown in Table 3. The Lewis acid sites of the Ni/Al-MCM-41 (WI) catalyst is greater than Ni/Al-MCM-41 (IWI) and Al-MCM-41 catalysts, resulting in higher conversion and yield. Increasing the Lewis acid sites can boost catalytic activity in the Reutealis trisperma oil deoxygenation reaction which correlated to the C–C bond breaking that occurs on the Lewis acid sites [17].

Table 3. Conversion, yield and degree of deoxygenation of liquid product

Catalysts	Conversion (%)	Yield (%)	Degree of Deoxygenation
Al-MCM-41	36.4	11.8	89.38
Ni/Al-MCM-41 (IWI)	49.0	16.1	91.10
Ni/Al-MCM-41 (WI)	55.4	20.1	92.77

Figure 5 depicts the distribution of hydrocarbon molecules resulting from the deoxygenation reaction. The deoxygenation reaction produces short chain hydrocarbons (C_{9-10}) and long chain hydrocarbons (C_{11-18}). The deoxygenation reaction using the Ni/Al-MCM-41(WI) catalyst generated a selectivity of hydrocarbon compounds (C_{11-18}) of 100%, with C_{15} and C_{17} hydrocarbons composition of 92.77%. The liquid product obtained by using Ni/Al-MCM-41 (IWI) catalyst produces selectivity of 95.33% for hydrocarbon compounds (C_{11-18}) and 4.67% for hydrocarbons (C_{9-10}) in with a major product selectivity of 81.01% for C_{15} and C_{17} hydrocarbons. The hydrocarbon selectivity (C_{9-10}) of Al-MCM-41 was 12.13%, and the hydrocarbon selectivity (C_{11-18}) was 87.87%.

All catalysts exhibit a dominant yield of C_{15} and C_{17} hydrocarbon chains which could raise the cetane number (CN) value as an indicator of fuel quality for ignition [28]. This suggests that the predominant reaction pathway in this reaction is the decarboxylation pathway. The decarboxylation route will result in straight chain alkanes with one less carbon atom than the original fatty acids and CO_2 gas as a by-product since Reutealis trisperma oil contains palmitic acid (C16:0), oleic acid (C18:1), and linoleic acid (C18:2) [17]. Therefore, a renewable, sustainable, and alternative biofuel, known as green diesel, is absolutely necessary to replace petroleum-based diesel and biodiesel in terms of effluent, no pollution, and economic attractiveness/cheapness, with the consumption of green diesel projected to increase to 3% annually in the upcoming 2030. Even the green diesel is regarded as the greenest, most economical, and potentially useful fuel to be utilized in diesel engines and produced on an industrial scale in the recent and future to minimize environmental pollution and to satisfy the rising diesel fuel demand [19].

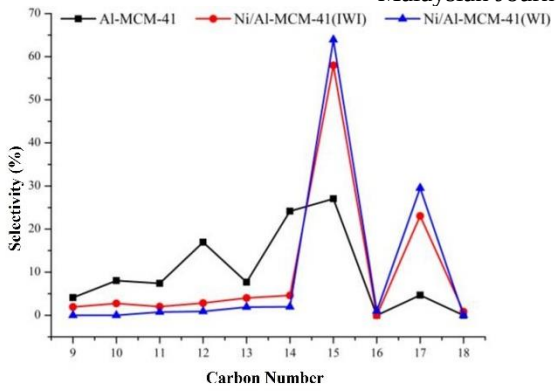

Figure 5. Hydrocarbon distribution from catalytic deoxygenation reaction of Reutealis trisperma oil

4. CONCLUSION

In this study, Al-MCM-41 and Ni/Al-MCM-41 has been successfully synthesized. All the catalysts show amorphous phase structure of MCM-41 and additional peak of NiO particle on Ni/Al-MCM-41. The NiO particle size on the Ni/Al-MCM-41 (WI) and NiAl-MCM-41 (IWI) catalysts were 55.5 nm and 83.4 nm. The Ni/Al-MCM-41 (WI) catalyst have the highest acid site with composition of Lewis acid of 0,196 mmol/g and Brønsted acid of 0.031 mmol/g. The Ni/Al-MCM-41 (WI) catalyst exhibited the highest hydrocarbon selectivity of 54.24% which was corroborated by the catalyst's high degree of deoxygenation in comparison to the Al-MCM-41 and Ni/Al-MCM-41 catalysts (IWI).

ACKNOWLEDGEMENTS

The authors acknowledge the Ministry of Research, Technology and Higher Education of Republic Indonesia under PDUPT research grant with contract number 1489/PKS/ITS/2022 and Universitas Pembangunan Nasional “Veteran” Jawa Timur under Riset Dasar scheme with contract number of SPP/108/UN.63. B/LT/V/2023 for funding the research.

REFERENCES

1. P. Balakrishnan, M.S. Shabbir, A.F. Siddiqi, X. Wang, Energy Sources, **42** (2020) 2698–2703.
2. N. Hongloi, P. Prapainainar, C. Prapainainar, Review of green diesel production from fatty acid deoxygenation over Ni-based catalysts, Molecular Catalysis **523** (2021) 111696.
3. R. Sotelo-boyás, F. Trejo-zárraga, F. de J. Hernández-Loyo, Hydrogenation, IntechOpen, 2012: 187–216.
4. N. Asikin-Mijan, H. V Lee, G. Abdulkareem-alsultan, A. Afandi, Journal of Cleaner Production **167** (2017) 1048–1059.
5. G.A. Alsultan, N. Asikin-Mijan, H. V. Lee, A.S. Albazzaz, Y.H. Taufiq-Yap, Energy Conversion Management, **151** (2017) 311–323.
6. N. Asikin-Mijan, H. V. Lee, J.C. Juan, A.R. Noorsaadah, H.C. Ong, S.M. Razali, Y.H. Taufiq-Yap, Applied Catalysis A: General **552** (2018) 38–48.
7. N.A.A. Rahman, J. Fermoso, A. Sanna, Fuel Processing Technology **173** (2018) 253–261.
8. W. Bambang, G. Guan, J. Rizkiana, X. Du, X. Hao, Z. Zhang, A. Abudula, Bioresources Technology **179** (2015) 518–523.
9. M.Y. Abduh, Syaripudin, L.W. Putri, R. Manurung, Energy Reports. **5** (2019) 1375–1380.
10. R.W. Gosselink, S.A.W. Hollak, S.W. Chang, J. Van Haveren, K.P. De Jong, J.H. Bitter, D.S. Van Es, ChemSusChem. **6** (2013) 1576–1594.
11. K.W. Jeon, H.S. Na, Y.L. Lee, S.Y. Ahn, K.J. Kim, J.O. Shim, W.J. Jang, D.W. Jeong, I.W. Nah, H.S. Roh, Fuel **258** (2019) 116179.
12. A. Veses, B. Puértolas, J.M. López, M.S. Callén, B. Solsona, T. García, ACS Sustainable Chemistry & Engineering, **4** (2016) 1653–1660.
13. M. Choo, L.E. Oi, T.C. Ling, E. Ng, Y. Lin, G. Centi, J.C. Juan, Journal of Analytical and Applied Pyrolysis, **`47** (2020) 104797.
14. F.P. Sousa, L.N. Silva, D.B. de Rezende, L.C.A. de Oliveira, V.M.D. Pasa, Fuel **223** (2018) 149–156.
15. K. de Sousa Castro, L. Fernando de Medeiros Costa, V.J. Fernandes, R. de Oliveira Lima, A. Mabel de Morais Araújo, M.C. Sousa de Sant’Anna, N. Albuquerque dos Santos, A.D. Gondim, RSC Advances **11** (2021) 555–564.
16. K.B. Baharudin, Y.H. Taufiq-Yap, J. Hunns, M. Isaacs, K. Wilson, D. Derawi, Microporous Mesoporous Materials, **276** (2019) 13–22.
17. R.E. Nugraha, D. Prasetyoko, H. Bahruji, S. Suprapto, N. Asikin-Mijan, T.P. Oetami, A.A. Jalil, D.-V.N. Vo, T.-Y. Yun Hin, RSC Advances, **11** (2021) 21885–21896..
18. R.E. Nugraha, D. Prasetyoko, N. Asikin-Mijan, H. Bahruji, S. Suprapto, Y.H. Taufiq-Yap, A.A. Jalil, Microporous Mesoporous Materials, **315** (2021) 110917.
19. H.I. Mahdi, A. Bazargan, G. McKay, N.I.W. Azelee, L. Meili, Chemical Engineering Research and Design, **174** (2021) 158–187.
20. F. Guo, J. Li, W. Li, X. Chen, H. Qi, X. Wang, Y. Yu, Quinoline Russian Journal of Applied Chemistry, **90** (2017) 2055–2063.
21. C. Huo, J. Ouyang, H. Yang, Scientific Reports, **4** (2015).
22. J. Xu, P. Xia, F. Guo, J. Xie, Y. Xia, H. Tian, Internationa Journal of Hydrogen Energy, **45** (2020) 30484–30495.
23. S. Qiu, X. Zhang, Q. Liu, T. Wang, Q. Zhang, L. Ma, Catalysis Communication, **42** (2013) 73–78.
24. F. Sahel, F. Sebih, S. Bellahouel, A. Bengueddach, R. Hamacha, Research on Chemical Intermediates, **46** (2020) 133–148.

25. S. Bailleul, I. Yarulina, A.E.J. Hoffman, A. Dokania, E. Abou-Hamad, A.D. Chowdhury, G. Pieters, J. Hajek, K. De Wispelaere, M. Waroquier, J. Gascon, V. Van Speybroeck, Journal of the American Chemical Society, **141** (2019) 14823–14842.
26. X. Li, D. Han, H. Wang, G. Liu, B. Wang, Z. Li, J. Wu, Fuel. **144** (2015) 9–14.
27. H. Li, Y. Wang, F. Meng, H. Chen, C. Sun, S. Wang, RSC Advances, **6** (2016) 99129–99138.
28. S.K. Bhatia, R. Gurav, T.R. Choi, H.R. Jung, S.Y. Yang, H.S. Song, Y.G. Kim, J.J. Yoon, Y.H. Yang, Energy Conversion Management, **192** (2019) 385–395.